Peer-reviewed version available at *Fluids* **2018**, *3*, 4; doi:10.3390/fluids3010004

Article

Computational Modelling for Efficient Transdentinal Drug Delivery

Agathoklis D. Passos[1], Dimitris Tziafas[2], Aikaterini A. Mouza[1], Spiros V. Paras*[1]

[1] Department of Chemical Engineering, Aristotle University of Thessaloniki, Greece
[2] Hamdan Bin Mohamed College of Dental Medicine, DHCC Dubai, UAE
* Correspondence: paras@auth.gr; Tel.: +30 2310 996174

Abstract: This work deals with the numerical investigation of the delivery of potential therapeutic agents through dentinal discs (i.e. a cylindrical segment of the dentinal tissue) towards the dentin-pulp junction. The aim is to assess the main key features (i.e. molecular size, initial concentration, consumption rate, disc porosity and thickness) that affect the delivery of therapeutic substances to the dental pulp and consequently to define the necessary quantitative and qualitative issues related to a specific agent before its potential application in clinical practice. The CFD code used for the computational study is validated with relevant experimental data obtained using micro Laser Induced Fluorescence (μ-LIF) a non-intrusive optical measuring technique. As the phenomenon is diffusion dominated and strongly dependent on the molecular size, the time needed for the concentration of released molecules to attain a required value can be controlled by their initial concentration. Finally, a model is proposed which, given the maximum acceptable time for the drug concentration to attain a required value at the pulpal side of the tissue along with the aforementioned key design parameters, is able to estimate the initial concentration to be imposed and vice versa.

Keywords: drug delivery; dentine; diffusion; bio-active molecules; CFD; μ-LIF; microfluidics

1 Introduction

During the last decades the clinical practice has been oriented towards the design and development of modern **dental treatment** techniques that would ensure the long-term maintenance of vitality and function of the dentine–pulp complex [1]. The traditional treatment strategies in vital pulp therapy have been mainly focused on protection of dental pulp from possible irritation presented by components released from dental materials and induction of replacement of diseased dentin by a layer of tertiary dentine [2]. Furthermore, the fact that the pulp-dentin complex can be repaired and as a part of reparative events tertiary dentin is formed, has recently led the scientific community towards the development of novel optimal procedures and production of potential therapeutic agents for use in regenerative pulp therapies. There is a growing weight of evidence that bioactive molecules diffused through the dentinal tubules can regulate the biosynthetic activity of pulpal cells [3-5]. The idea of using the dentinal **tubules**, i.e. structures running in parallel the whole thickness of dentin, for drug delivery in pulp was originally proposed by Pashley, D.H. [6]. Later Pashley, D.H. [7] suggested that the therapeutic agents must consist of small molecules or ions that exhibit relatively high diffusion coefficients.

Since it is known that a remaining dentin zone (Remaining Dentin Thickness, RDT) is necessary to protect the dental pulp survival and function [8], much has still to be learnt on the effect of potent toxic components that are released from traditional restorative materials or bioactive signaling molecules, the promising basis of novel regenerative therapeutic applications. It is reasonable to suggest that any toxic interruption of pulp functions or therapeutic up-regulation of, the responsible for the biosynthetic activity of teeth, odontoblasts will probably reflect the molecular concentration of these constituents at the dentin-pulp interface area [9]. Thus, a number of delivery considerations might be firstly addressed.

Peer-reviewed version available at Fluids 2018, 3, 4; doi:10.3390/fluids3010004

However, due to the minute dimensions of the dentinal tubules, the experimental study of the drug delivery through the dentinal tubules under the same conditions as in clinical therapy is practically impossible using the established experimental techniques. In this case, the development of novel techniques would permit the prediction of the transport rate of selected therapeutic molecules.

Several in vitro experimental studies reported in the literature concern the inward diffusion of substances in dentinal slabs that are placed in custom made split-chamber devices under the absence/existence of simulated pulpal pressure. Pashley, D.H.,Matthews, W.G. [10] conducted experiments aiming to evaluate the influence of outward forced convective flow on the inward diffusion of radioactive iodide. In addition Hanks, C.T., Wataha, J.C. [11] investigated the diffusion through dentine by a number of biological and synthetic molecules, including resin components and dyes. However, due to limitations imposed by the experimental techniques, these studies fail to fully represent the actual tooth case and can only provide information concerning the permeability of several substances through dentinal discs. Several equations derived from Fick's Second Law of diffusion are proposed in the literature for the theoretical study of the flow through a tubulus, but due to the non-uniformity of the cross-section of dentinal tubules the theoretical equations are difficult to apply. Consequently, Computational Fluid Dynamics (CFD) appears to be the most feasible method for studying the problem under consideration. Several studies confirmed that CFD is a powerful analytical tool in dental pulp research [e.g. 12-14]. The simple case that concerns delivery of bioactive therapeutic agents to the dentin-enamel junction (DEJ) through a typical dentin tubule that has no obstructions or alterations of any type has been numerically studied in our Laboratory [15]. The results of this initial approach led to the formulation of a simplified model that is able to estimate the initial drug concentration to be imposed when a given type of therapeutic molecules are transported through a **single** and enclosed dentinal tubule.

The present work extends our previous study by numerically investigating the delivery of potential therapeutic agents towards the dentin-pulp junction in enclosed cavities not only through a single dentine tubule but through dentinal **discs** (i.e. a cylindrical segment of the dentinal tissue) by addressing new key design parameters (i.e. Remaining Dentin Thickness, Porosity and Consumption Rate) in a way that fully represents the actual tooth case. The study will also include the effect of the number of the active dentinal tubules expressed by a porosity value as well as the effect of the dentin-pulp barrier expressed as a consumption rate at the pulp on the drug delivery characteristics.

2 Transport of therapeutic compounds through the dentinal tissue

Dentin is a mineralized matrix that is porous and yellow-hued. It is made by up of 70% inorganic materials (mainly hydroxyapatite and some non-crystalline amorphous calcium phosphate), 20% organic materials (90% of which is collagen type 1 and the remaining 10% ground substance, which includes dentine-specific proteins), and 10% water [16]. The dentin tissue consists of microscopic channels, called **dentinal tubules**, which radiate outwards through the dentin from the pulp to the exterior cementum or enamel border. Figure 1 gives a typical representation of the tissues that form a human tooth (Figure 1a & 1b) and the dentinal tubules (Figure 1c). In the tooth crown, the dentinal tubules extend from the dentino-enamel junction (DEJ) to the pulp periphery following an *S*-shaped path. Tapering from the inner to the outermost surface, they have an average diameter of 2.5 μm near the pulp, 1.2 μm in the middle of the dentin, and 0.9 μm at the DEJ, while the total tissue width is estimated to be about 2.5 mm [17]. Most of the dentinal tubules contain non-myelinated terminal nerves and odontoblasts that are placed in an environment filled with dentinal fluid [18-20].

The tubule density and diameter at various levels defines the surface area occupied by tubules. More specifically, the area of dentin occupied by tubules at the dentino-enamel junction is only 1% and increases to 45% at the pulp chamber [16]. Their density is 59,000 to 76,000 tubules/mm^2 near the pulp. In addition, there are branching canalicular systems that connect to each other. The number of dentinal tubules per unit area varies according to the age and the gender of each individual.

Preprints (www.preprints.org) | NOT PEER-REVIEWED | Posted: 14 November 2017 doi:10.20944/preprints201711.0090.v1

Peer-reviewed version available at Fluids 2018, 3, 4; doi:10.3390/fluids3010004

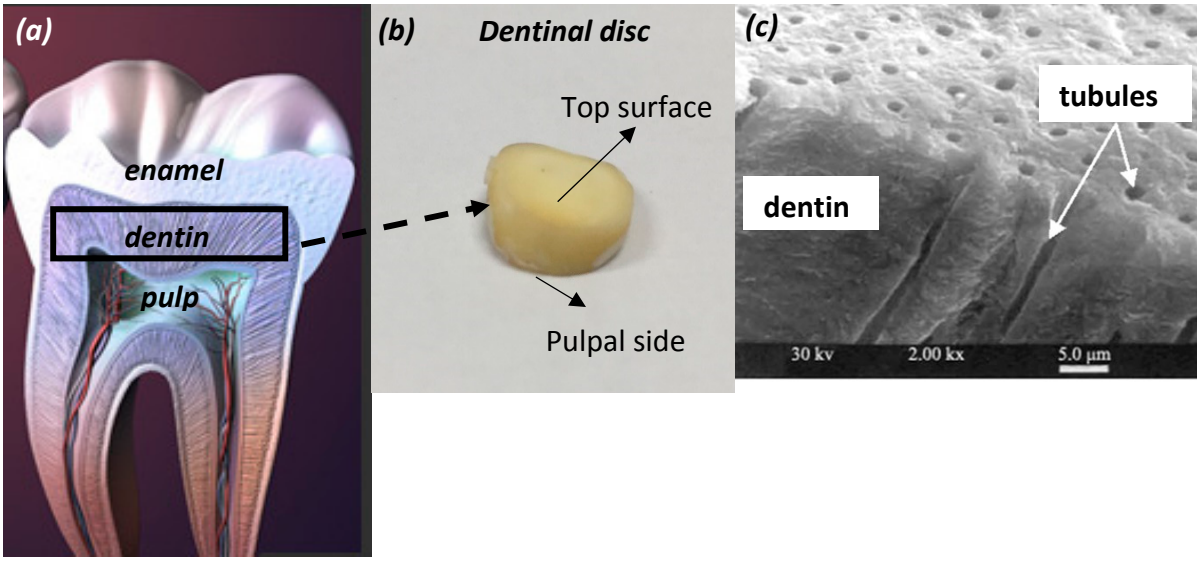

Figure 1: (a) Typical cut-away representation of human tooth; (b) and (c) Dentinal tubules running perpendicularly from pulpal wall towards DEJ [21].

In clinical practice, when the dentin pulp complex is affected by caries or trauma, biological compounds are placed in enclosed cavities and then diffuse through the dentinal fluid to the pulp. In the dental practice the fluid outflow is avoided by covering the surface of traumatized dentin tissue with suitable dental materials after the addition of the therapeutic agent. On the contrary, in cases of open cavities, compounds/bacteria and even therapeutic agents that are placed in the vicinity of the cavity may never enter the dentinal tubules due to the resistance of the dentinal fluid outflow.

In the framework of the present computational study the dentinal tissue is modeled as a porous disc with tortuosity value τ=1.The transport of substances in a cylindrical section of the tissue is investigated under the effect of the geometrical characteristics of the tissue, the size and initial concentration of the applied molecules as well as their consumption rate at the pulpal side of the tooth.

3 Materials & Methods

3.1 Code Validation

Prior to proceeding to the computational procedure, the CFD simulations were validated using experimental data acquired by performing **experiments** using dentinal porous discs. The dentinal discs employed were 0.85±0.05 mm thick (Figure 1b) and were cut perpendicular to the vertical axis of exported human teeth, just above the level of the pulp horns, by a low speed saw ISOMET (Buehlel, USA) under constant water coolant were. The dentine discs were hand-sanded under tap water, by a 600-grit silicon carbide paper to achieve a uniform flat surface with smear layer, acid-etched on both sides, with 35% phosphoric acid (Ultra etch, Ultradent, USA) for 15 secs and then thoroughly rinsed with water spray in order to clean the disc and remove the smear layer from the dentine. The disc was placed between two transparent glass tubes with a standard central hole (32 mm^2) and it was attached with a minimum quantity of aquarium marine silicone (Top sil, Mercola, Athens) placed carefully peripherally, to the enamel margins of the dentine disc. After the silicone was set, all the joins were reinforced externally with sticky wax (Kem-den, Purton, England) and the whole system was filled with Ringer's solution (Vioser, Greece) to be checked for leakages. The experimental conduit is shown schematically in Figure 2**.** The conduit was constructed at the Dental School of Aristotle University of Thessaloniki.

Rhodamine B is a fluorescent dye with a quantum yield of up to ϕ=0.97 at low concentrations. The diffusion of Rhodamine B in an aqueous solution through the dentinal disc to the opposite area (i.e. the observation area) is measured using the non-intrusive experimental technique μ-LIF (μ-Laser Induced Fluorescence). Two concentration groups of the aqueous solution were used, namely **G1** for M_0=0.1 mg/L and **G2** for M_0=0.05 mg/L.

Preprints (www.preprints.org) | NOT PEER-REVIEWED | Posted: 14 November 2017 doi:10.20944/preprints201711.0090.v1

Peer-reviewed version available at Fluids 2018, 3, 4; doi:10.3390/fluids3010004

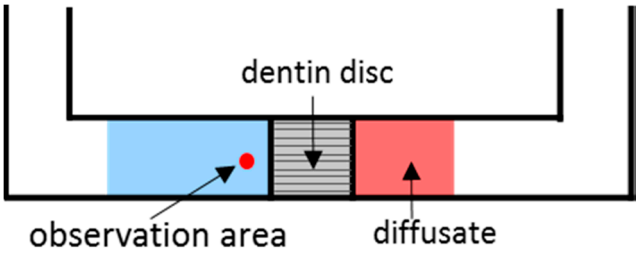

Figure 2: Test section of the experimental conduit.

The μ-LIF experimental setup, available in our Lab, is shown in Figure 3. The measuring section was illuminated by a double cavity Nd:YAG Laser emitting at 532nm. The fluid flux was measured by a high sensitivity CCD camera (Hisense MkII), connected to a Nikon (Eclipse LV150) microscope, which moves along the vertical axis with an accuracy of one micron. A 10X air immersion objective with NA=0.20 was used. For each measurement, at least 20 images were acquired at a sampling rate of 5 Hz.

The experiments were performed using two liquids, namely distilled water as reference and distilled water marked with the fluorescent dye Rhodamine B, completely dissolved in water, whose diffusion coefficient in water is $4.5 \cdot 10^{-10}$ m^2/s [22]. As reported by Bindhu, C.V.,Harilal, S.S. [23] Rhodamine B quantum yield depends on the solvent and on the type of excitation (continuous, pulsed) and decreases weakly with increasing concentration. Rhodamine B, dissolved in water, is most effectively excited by green light and emits red light with the maximum intensity in the range 575–585 nm [23, 24]. Image processing and concentration calculations were performed using appropriate software (Flow Manager by Dantec Dynamics).

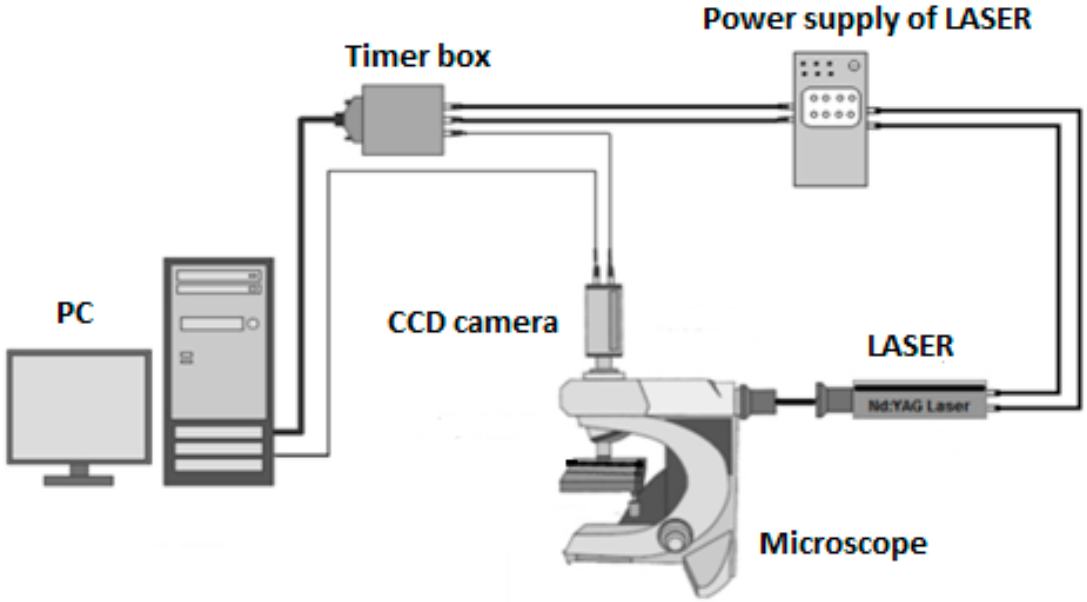

Figure 3: μ-LIF experimental setup.

A typical procedure for μ-LIF measurements consists of the following steps:

- Determination of the **relationship** between the measured fluorescence intensity field $I_{(x,t)}$ and the concentration field $C_{(x,y)}$.
- Calibration experiments prior to the actual measurements using a series of aqueous Rhodamine B solutions with known concentrations, namely M=0.05, 0.025 and 0.00 mg/L. For each concentration C_i an image $C_{(x,y)}$ is taken.
- Image masking of the acquired images is also necessary in order to reduce noise and then an appropriate Region of Interest (ROI) is defined, at which the fluorescence intensity is measured.

Preprints (www.preprints.org) | NOT PEER-REVIEWED | Posted: 14 November 2017 doi:10.20944/preprints201711.0090.v1

Peer-reviewed version available at Fluids 2018, 3, 4; doi:10.3390/fluids3010004

For our experiments, the optical system was set to have a ROI of 300x580 μm, while the lens was focused on the middle plane of the capillary. Care was taken to ensure that the experiments are conducted at identical conditions with the calibration procedure, so as to minimize the uncertainty of the experimental procedure. The uncertainty of the method is estimated to be less than ±5% [25]. Finally, concentration measurements were performed on the middle plane, at the observation area (Figure 2), namely at most 1 mm from the pulpal side of the dentinal disc. As there is no lateral diffusion, i.e. the process is 1D, we can assume that the concentration is constant along the diameter of the tube. Thus, the μ-LIF measurement corresponds to the mean concentration at a cross-section of the conduit.

The processing of the μ-LIF images comprises:

- the definition of the mean image out of a set of 20 images and
- the comparison of each mean image with the μ-LIF calibration curve that has been previously created.

The porosity of the dentin disc was measured using Scanning Electron Microscopy (SEM). Apart from the experimental measurements we also performed computational simulations. A computational domain that fully represents the experimental setup was designed and the numerical results were compared with the corresponding experimental ones. This comparison is presented in Figure 4, where the temporal concentration value of Rhodamine B at the observation area is measured for a dentinal disc with porosity ϕ=10%.

The comparison of the CFD data with the available experimental results indicate a very good agreement, i.e. better than ±15%. Consequently, the CFD code can be considered suitable for performing additional simulations concerning the transport of substances through the porous disc.

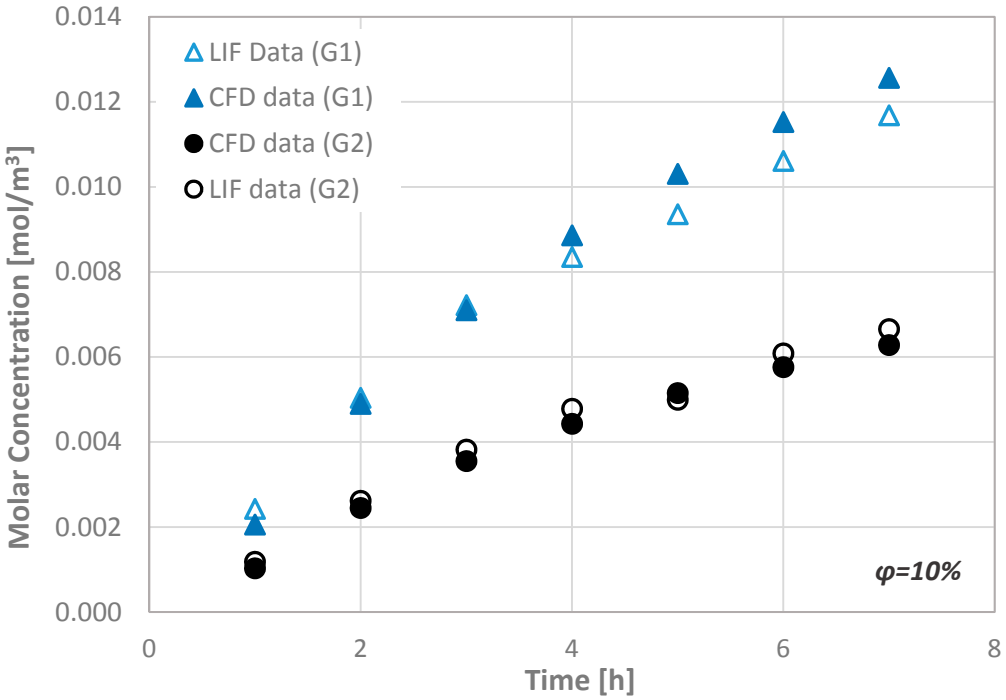

Figure 4: Typical comparison of the molar concentration values at the observation area of the μ-LIF technique with the corresponding computational results (ϕ=10%).

3.2 Numerical Procedure

In this study, we aim to investigate the delivery of potential therapeutic substances placed at the top surface of the dentinal tissue to the pulpal side by molecular diffusion through the dentinal fluid that occupies the micro-pores of the tissue. In order to accomplish this, we assume that dentine is a porous tissue with a porosity value related directly to the volume of dentinal fluid per unit volume of the tissue. Since the porosity of the dentin tissue is generally unknown and its thickness, especially in cases of traumatized teeth, is variable, we performed a **parametric** study that incorporates the effect of these two parameters on the diffusion process characteristics. In addition, the present parametric study

Preprints (www.preprints.org) | NOT PEER-REVIEWED | Posted: 14 November 2017 doi:10.20944/preprints201711.0090.v1

Peer-reviewed version available at Fluids 2018, 3, 4; doi:10.3390/fluids3010004

includes the effect of the consumption of the diffusates at the pulpal side of the dentinal tissue, where the odontoblasts are located. The consumption at the pulpal side of the dentinal tissue is modeled by employing a **constant** consumption rate of the diffusate. Since the consumption rate of the agents is considered unknown, we employed a range of consumption rates between 0 (i.e. no consumption is assumed) and 10^{-10} kg/(m^2·s). Finally, a parametric study is performed that includes the effect of:

- the porosity of the tissue (ϕ),
- the thickness of the tissue (Remaining Dentinal Thickness, *RDT*),
- the initial concentration (M_0) of the substances to be diffused,
- their molecular size, i.e. their Diffusion Coefficient and
- the consumption rate (R) of the diffusate at the pulpal side

on the transport characteristics through an **enclosed** dentinal disc.

The porous disc is considered to be initially full with dentinal fluid, i.e. a fluid that has the thermophysical properties of water. In Figure 5 the computational domain is schematically presented. The disc is cylindrical with a cross-section area of 32 mm^2, while the diffusate occupies a volume of 32 mm^3.

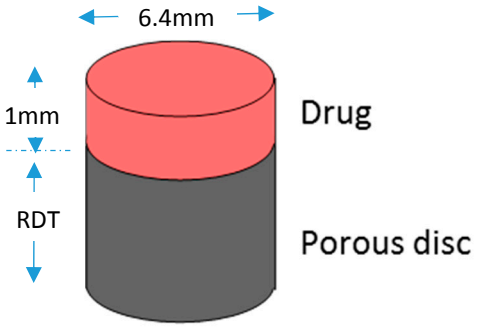

Figure 5: Computational domain for the porous disc model. (RDT=0.5-2.5mm)

The permeability of porous media is usually expressed as function of some physical properties of the interconnected system, such as porosity and tortuosity. Although it is natural to assume that permeability values depend on porosity, an appropriate relationship is not simple to be determined, since this would require a detailed knowledge of size distribution and spatial arrangement of the pore channels in the porous medium. For instance, two porous systems can have the same porosities but different permeabilities. One of the most widely accepted and simplest model for the permeability-porosity relationship is the Kozeny-Carman (KC) model, which provides a link between media properties and flow resistance in pore channels. In this study we apply the general Poiseuille equation in a straight channel with a generic cross-sectional shape [26]:

$$U_{channel} = -\frac{A}{a}\frac{1}{n}\frac{dp}{dx} \quad (1)$$

where A is the generic cross-sectional area of the micro-channel and a is a dimensionless geometric factor. Classical derivations of the KC model [27, 28] consider the case of a circular cross-section as a starting point in Eq. 1, i.e. $A/a = R^2/8$. They extend and adapt Eq. 1 to the equivalent channel model of the porous body by taking into the effects of (i) the effective tortuous path, (ii) the effective volume and (iii) the concept of effective radius R:

$$U = -c\frac{R^2}{8}\frac{\varphi}{\tau}\frac{1}{n}\frac{dp}{dx} \quad (2)$$

where c (=2 for cylindrical micro-pores) was introduced as an empirical geometrical parameter, ϕ is the porosity, τ the tortuosity defined as the square of the ratio between the effective channel length L_e due to the tortuous path and the length L of the porous body ($\tau \equiv L_e/L$). Comparison of Eq. 2 with Darcy's law gives the following expression for defining the permeability (k) (Eq. 3):

$$k = c\frac{R^2}{8}\frac{\phi}{\tau} \quad (3)$$

To study the diffusion process, we employ substances, whose molecular sizes are the same as those of proteins or therapeutic agents used in dental clinic practice. The radius R_{min} and the diffusion coefficient D of a protein can be estimated by Eqs. 4 & 5 [29].

$$R_{\min} = 0.066 M_w^{1/3} \quad (4)$$

where R_{min} is given in nanometers and the molecular weight M_w in Daltons (Da) and

$$D = \frac{kT}{6\pi\mu R_s} \quad (5)$$

where $k = 1.38\times10^{-16}$ g·cm²·s⁻²·K⁻¹ is the Boltzmann constant and T the absolute temperature. k is given here in centimeter–gram–second units because D is expressed in centimeter–gram–second, while μ that stands for the solute viscosity is in g/(cm·s), which in our case is assumed to be that of water as its thermophysical properties are very close to those of the actual dentinal fluid [30]. R_s, called Stokes radius, represents the radius of a smooth sphere that would have the same frictional coefficient f with a protein and is expressed in centimeters in this equation. Assuming that f equals f_{min}, i.e. the minimal frictional coefficient that a protein of a given mass would obtain if the protein were a smooth sphere of radius R_{min}, R_s can be replaced by R_{min} in Eq. 5**.**

In this study **three different** diffusates are considered, which cover a wide range of molecular sizes that correspond to the size of actual bioactive molecules. The radius R_s of the molecules tested is in the range of 2.2-22.0 nm and consequently the corresponding diffusion coefficient, D, in water at 37 C, is in the range of $1.36\text{-}0.14\cdot10^{-10}$ m²/s. For example, BMP-7 is a bioactive protein used in the dental clinic practice with approximately 50 kDa molecular weight and R_s of 2.2 nm. To conduct a parametric study, three initial mass concentration values for each diffusing substance are employed, i.e. 0.10, 0.05 and 0.01 mg/mL.

The parametric study was performed using **three** porosity values (ϕ), namely 5%, 10% and 20% which can be regarded to adequately represent the porosity values of the dentin tissue as it can be seen from Section 2. Employing the Design Exploration features of ANSYS Workbench® package and following the Design of Experiments (DOE) methodology, a set of "computational experiments" has been initially designed. The DOE methods allow the designer to extract as much information as possible from a limited number of test cases and makes the method ideal for CFD models that are significantly time-consuming [31]. A summary of the design variable ranges is given in Table 1**.**

Table 1: Constraints of the design variables.

Parameter	Lower bound	Upper bound
Porosity (ϕ), %	5	20
Remaining Dentinal Thickness (RDT), mm	0.5	2.5
Initial Concentration (M_0), mg/mL	0.01	0.10
Molecular Size (R_s), nm	2.2	22.0
Consumption Rate (R), kg/(m²·s)	0	10^{-10}

A grid dependency study was also performed for the case involving the diffusate with the highest diffusion coefficient value. This leads to the construction of an unstructured mesh of $1\cdot10^6$ of tetrahedral elements, while the porosity model is used to account for the space occupied by dentinal tubules per unit area in the disc. All simulations were run in transient mode, while the total simulation time for each run varied in the range of 10-25 h, depending on the consumption rate (R) applied. A time-step dependency study was also performed (i.e. time steps in the range of 5–10 s). Zero flux was applied at all the walls of the computational domain as boundary conditions, while when a consumption rate is

employed, negative flux is imposed at the pulpal side. For the discretization scheme, the High Resolution one was employed and as for the transient scheme, a Second Order Backward Euler scheme was used. A high-performance unit for parallel computing is employed which runs on a Gentoo Linux distribution.

4 Results

Since the behavior observed among the numerous computational results of the present study is similar, only **typical** examples of the effect of each key design parameter on the molar concentration at the pulpal side of the dentinal discs (C_L) are presented. Accordingly, and for the sake of clarity, the general case where a consumption rate is imposed at the pulp is shown first, while for the results presented concerning the other parameters, **no consumption** is assumed, i.e. R=0.

4.1 Effect of the agent consumption rate at the pulpal side

Figure 6 shows the concentration at the pulpal side for different consumption rates applied when an agent with R_s=2.2 nm & M_0=0.10 mg/mL is employed at the top of the dentinal disc of ϕ=10%. As it can be seen the concentration value at the pulpal side is lower than the initial one regardless of the consumption rate applied. The concentration value may exhibit 100% reduction when the lowest and the highest consumption rates are compared. During the first time steps of the agent application on the disc, the concentration gradient along the disc thickness is significantly high and the concentration at the pulpal side C_L increases until t^*=1 (i.e. dashed line). In the cases where the agents are consumed and after this critical time steady-state equilibrium cannot be reached. On the contrary, as time passes, the agent is being continuously consumed, which means that the concentration at the pulp will decrease until the agent disappears.

It is expected that after few hours the tissue will be free of the agent presence. The total estimated time for this to happen depends on the applied consumption rate that is imposed, the porosity of the dentinal disc and the initial concentration. For a consumption rate of 10^{-10} kg/(m^2·s) the total estimated time for an agent of R_s=2.2 nm to be fully consumed is approximately 18 hours in a porous disc of ϕ=10%.

From Figure 6 becomes evident that the consumption rate of the therapeutic agent does not affect the form of the curve but only the magnitude of the C_L values. Given that and in order to facilitate the evaluation of the effect of the other parameters, zero consumption rate at the pulp end is assumed for the remaining CFD simulations.

4.2 Effect of Remaining Dentin Thickness (RDT)

The effect of the remaining dentin thickness (RTD) on the concentration at the pulpal side (C_L) is shown in Figure 7**,** when a substance of R_s=4.4 nm at M_0=0.10 mg/mL is diffused through a dentinal disc of ϕ=5%. As it is expected, since the process is considered one-dimensional, it is dominated by the diffusional length. For discs with significant low thickness the delivery of substances to the pulp is rapid and a steady state condition can be rather quickly achieved. For example, when a dentinal disc of 0.5 mm is employed the concentration at the pulpal side reaches its final value after two hours of application. The time barrier for steady state condition can be easily estimated from the dimensionless time variable $t=D/L^2$.

Preprints (www.preprints.org) | NOT PEER-REVIEWED | Posted: 14 November 2017 doi:10.20944/preprints201711.0090.v1

Peer-reviewed version available at Fluids 2018, 3, 4; doi:10.3390/fluids3010004

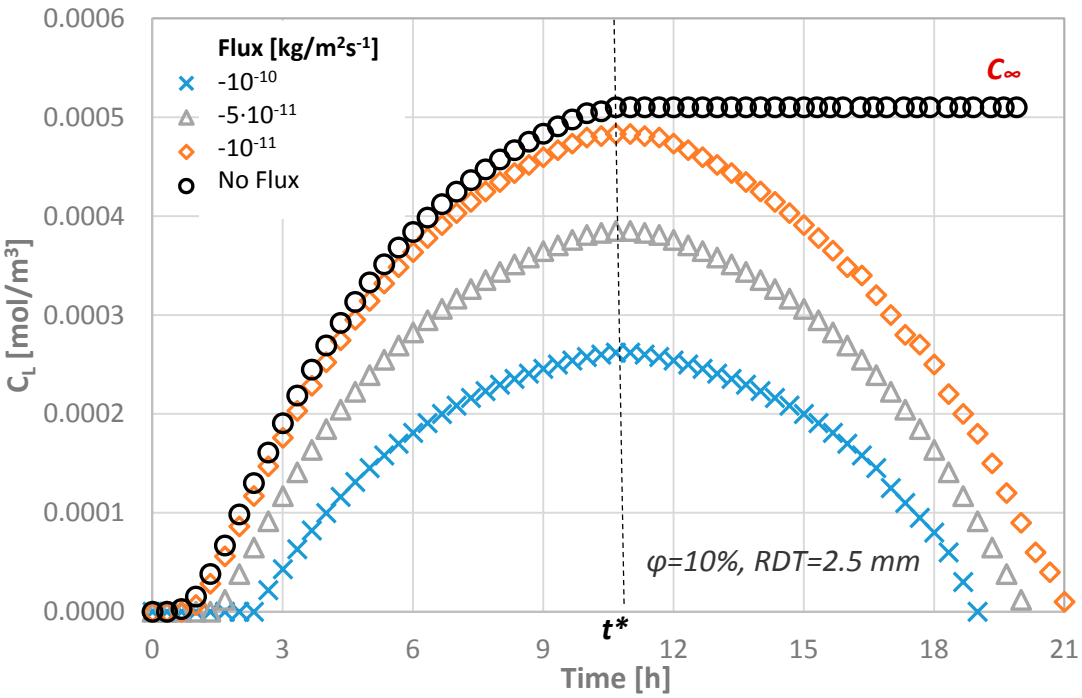

Figure 6: Molar concentration at the pulpal side of the dentinal discs as a function of different consumption rates for ϕ=10% and *RDT*=2.5 mm.

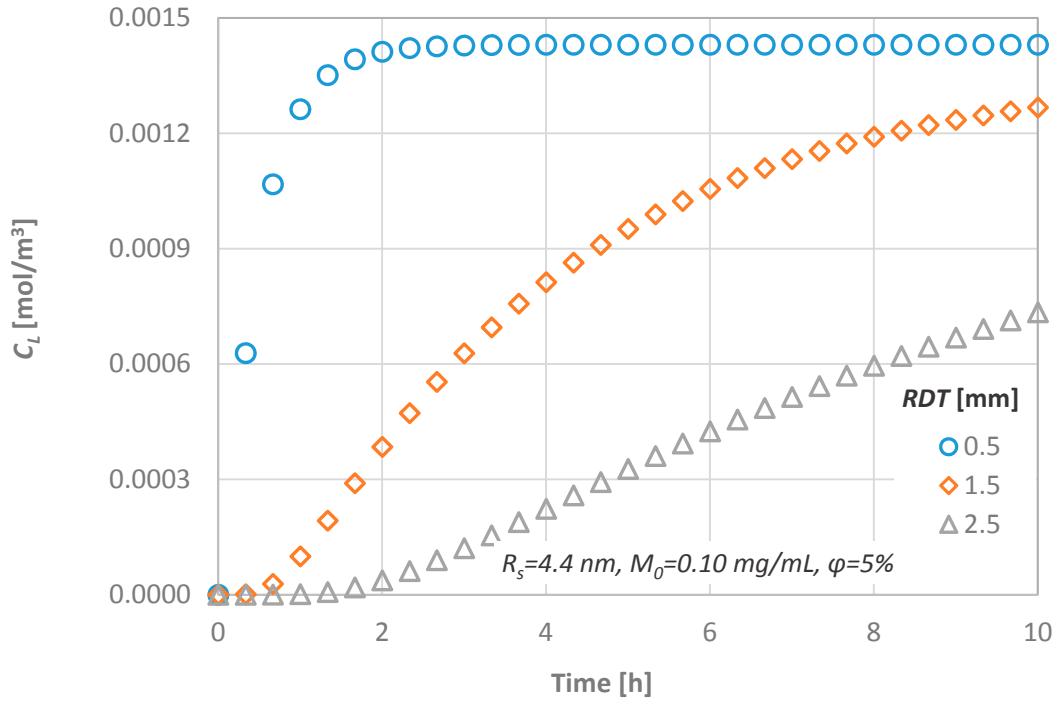

Figure 7: Effect of the *RDT* on the diffusion characteristics; C_L versus time.

Preprints (www.preprints.org) | NOT PEER-REVIEWED | Posted: 14 November 2017 doi:10.20944/preprints201711.0090.v1

Peer-reviewed version available at Fluids 2018, 3, 4; doi:10.3390/fluids3010004

In order to gain a greater insight into the transport process through dentinal discs, the temporal molar flux is calculated and presented in Figure 8. The magnitude of the diffusional flux across the dentinal tissue is inversely proportional to the dentine thickness, an observation that agrees with the relevant literature [10, 32].

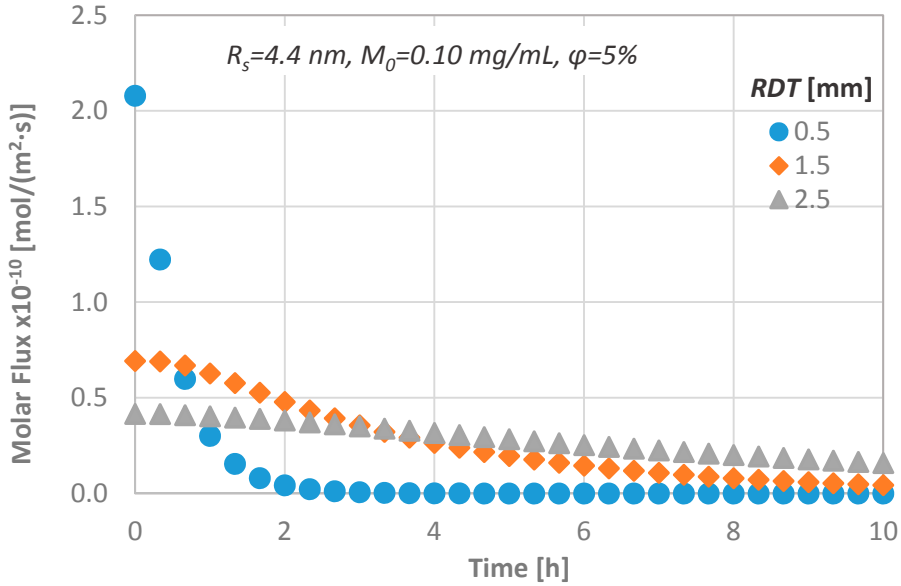

Figure 8: Effect of the *RDT* on the diffusion characteristics; Molar flux versus time.

4.3 Effect of the molecular size

For a given dentinal disc (i.e. same *RDT* & porosity) the diffusion is controlled by the diffusion coefficient of each diffusing agent, while the estimated final value will be the same in all cases. The concentration variation with time at the bottom end area is presented in Figure 9 for three substances with different molecular sizes. As it is expected, substances/proteins with larger molecules penetrate at a lower rate inside the disc, because their diffusion coefficient is a function of the size of the molecules as described in Section 3.2.

For the delivery of substances with different molecular sizes the concentration gradient inside the dentinal tissue is presented in Figure 10**.** The molar flux is greater during the middle steps of the process, as the substance penetrates at a greater rate inside the tissue. Obviously, the substances with greater molecular sizes diffuse at a lower rate through media and as it can also be seen from Figure 9 it needs more than 10 h for the concentration C_L of the substance with the greatest molecular size to reach steady state conditions (i.e. the concentration gradient to be zero).

4.4 Effect of dentine porosity

The calculated temporal concentration values of the diffusing agent at the pulpal side of the dentinal discs as a function of the porosity of the tissue are presented in Figure 11. As the porosity of the tissue decreases, higher values of concentration are observed at the pulpal side, because the available area for the substance to be diffused is reduced. However, the porosity of the discs does not affect the time needed for the steady state condition to be reached.

The variation in concentration at the pulpal side depends strongly on both the porosity and the dentin thickness. The results indicate that there is 5% difference between the minimum and the maximum *RDT* dentinal discs investigated in this study for low porosity values, i.e. 5%. As the total pore volume increases this difference increases too and reaches is upper limit of 15% for the dentin slab with the maximum thickness (i.e. *RDT*=2.5 mm).

Preprints (www.preprints.org) | NOT PEER-REVIEWED | Posted: 14 November 2017 doi:10.20944/preprints201711.0090.v1

Peer-reviewed version available at Fluids 2018, 3, 4; doi:10.3390/fluids3010004

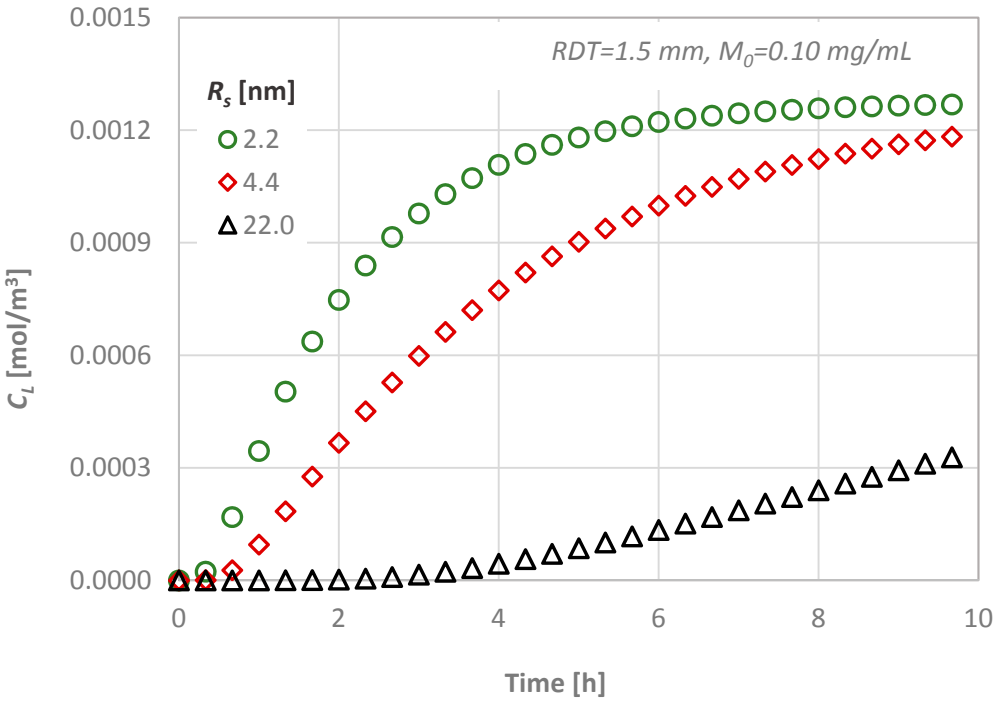

Figure 9: Effect of the molecular size on the diffusion characteristics; C_L versus time.

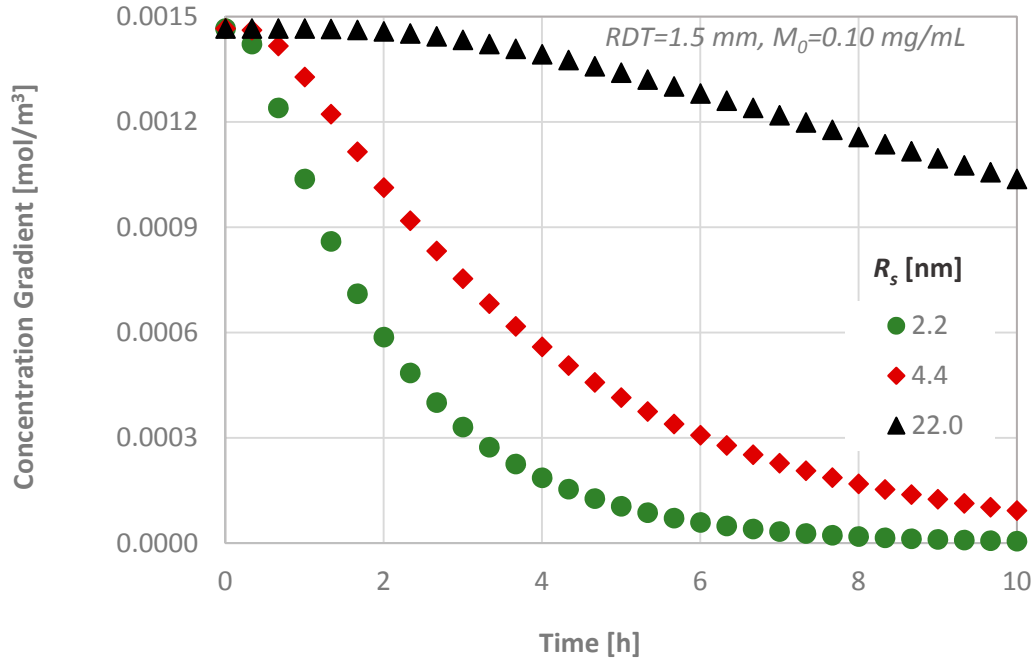

Figure 10: Effect of the molecular size on the diffusion characteristics; Concentration gradient versus time.

Preprints (www.preprints.org) | NOT PEER-REVIEWED | Posted: 14 November 2017 doi:10.20944/preprints201711.0090.v1

Peer-reviewed version available at Fluids 2018, 3, 4; doi:10.3390/fluids3010004

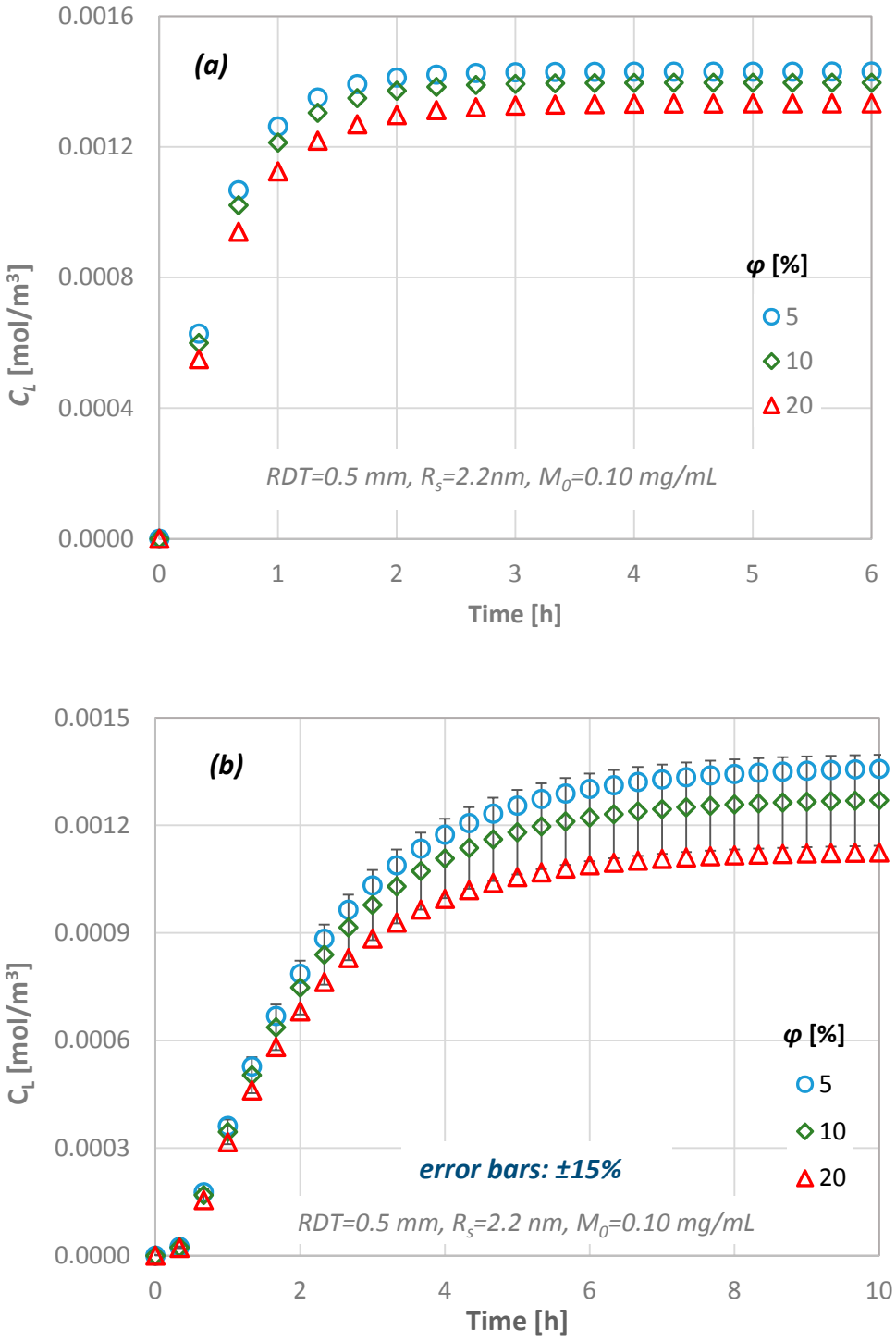

Figure 11: Effect of the dentinal disc porosity value on the diffusion characteristics for: (a) *RDT*=0.5 mm, R_s=2.2nm and (b) *RDT*=1.5 mm, R_s=2.2 nm.

In Figure 12 the flux for three different dentinal discs in terms of porosity values is presented, while the *RDT*, diffusion coefficient and initial substance concentration are kept constant (i.e. *RDT*=1.5 mm, R_s=4.4 nm and M_0=0.01 mg/mL). It can be observed that the different porosity values do not practically affect the calculated molar flux through the dentinal discs.

Preprints (www.preprints.org) | NOT PEER-REVIEWED | Posted: 14 November 2017 doi:10.20944/preprints201711.0090.v1

Peer-reviewed version available at Fluids 2018, 3, 4; doi:10.3390/fluids3010004

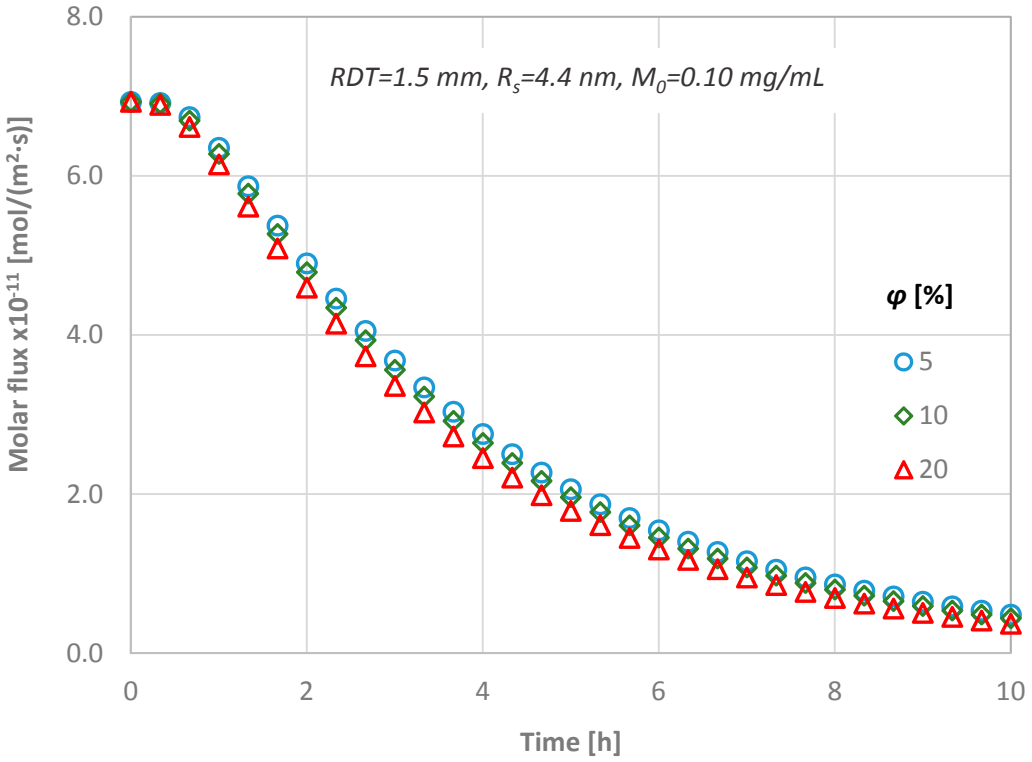

Figure 12: Temporal molar flux distribution for three different porous discs (RDT=1.5 mm, R_s=4.4 nm and C_0=0.10 mg/mL).

4.5 Effect of the initial diffusate concentration

The transport of a substance similar to the therapeutic agent BMP-7, through a dentinal disc of RDT=1.5 mm to the pulpal side under different values of initial concentration has been also studied. The calculated concentrations at the bottom of the disc C_L are presented in Figure 13**.** One can observe that, after approximately 0.5 h, the first molecules of the substance do reach the bottom end of a dentinal disc of 1.5 mm RDT. This is in accordance with the literature and especially with Pashley, D.H., Matthews, W.G. [10] who have reported that diffusion is a low process and, depending on their size, it requires 30-120 minutes for the molecules to reach the pulp across a 1-2 mm dentin thickness.

Obviously, the time required for the concentration of signaling molecules to attain a specific value at the bottom end is controlled by their initial concentration, i.e. by increasing the initial concentration of a potential therapeutic agent, the mass flux inside the disc increases and thus the signaling time of the molecules decreases (t_1 and t_2 in Figure 12). This is important for clinical practice of dentistry, since by this procedure the behavior of each therapeutic agent can be predicted prior to its application.

4.6 Prediction of the drug pulpal concentration

In an effort to obtain a generalized correlation concerning the delivery of agents through porous domains to the dental pulp that could simulate human dentin tissues, we employed and modified a previous proposed correlation [15] concerning the diffusion through a typical dentinal tubule (Eq. 6):

$$C_L/C_0 = 1.1\exp\left(\frac{0.115}{t^*}\cdot\ln(t^*)+10^{-3}L\right) \quad (6)$$

Eq. 6 is a simplified approach that predicts the temporal concentration distribution of the agent at the dentin-pulp junction in the **ideal case** where all dentinal tubules share the same geometrical characteristics and there is no agent consumption. However, one can speculate that this cannot always adequately represent the actual case. For this reason, a **new** correlation for the prediction of the diffusion characteristics through dentinal discs is formulated to include all the key design parameters investigated in the present study. In the case where agents are consumed in the pulp, the shape of the molar

Preprints (www.preprints.org) | NOT PEER-REVIEWED | Posted: 14 November 2017 doi:10.20944/preprints201711.0090.v1

Peer-reviewed version available at Fluids 2018, 3, 4; doi:10.3390/fluids3010004

concentration curvature is different from what it can be calculated through Eq. 6 where no flux (i.e. consumption of agents) is imposed at the bottom end of the dentinal tubules. The new equation is a **4th order polynomial** so as to take also into account the gradual decrease of the diffusate until its extinction. The new equation (Eq. 7) is:

$$C_L = C_0(10^{-10}R + 2.1)(125RDT + 1.3)0.11\varphi^{0.27}(1.1t^{*4} - 5t^{*3} + 4.9t^{*2} + 0.06t^{*} + 0.01) \quad (7)$$

where R is the consumption rate in kg/(m²·s) and RDT in m. The outcome of Eq. 7 has been compared with the available data from the computational simulations and the overall uncertainty is satisfactory (i.e. less than ±15%). Figure 14 presents this comparison when an agent of R_s=2.2 nm is transported through a 2.5 mm thick dentinal disc of ϕ=10% for M_0=0.10 (Figure 14a) & 0.05 (Figure 14b) mg/mL, respectively.

If there is no consumption of the agent, Eq. 7 is valid for $t^*\leq 1$ (at the maximum C_L). Eq. 7 permits the estimation of the necessary initial concentration of the therapeutic agent for an efficient therapy, i.e. the drug concentration at the pulp to reach a **critical** signaling value dictated by the dental clinical practice, when the maximum acceptable time of application and the consumption rate are given. From Figure 14 it can be observed that there is always a time margin during which the agent attains its maximum value at the pulp (i.e. ~2 h in the specific case of Figure 14). However, since the R values have been arbitrarily chosen, the scientific community that deals with phenomena related with the dental pulp irrigation and dentinal tissue regeneration must **quantify** the desirable consumption rate of biomolecules/proteins in the vicinity of the pulp.

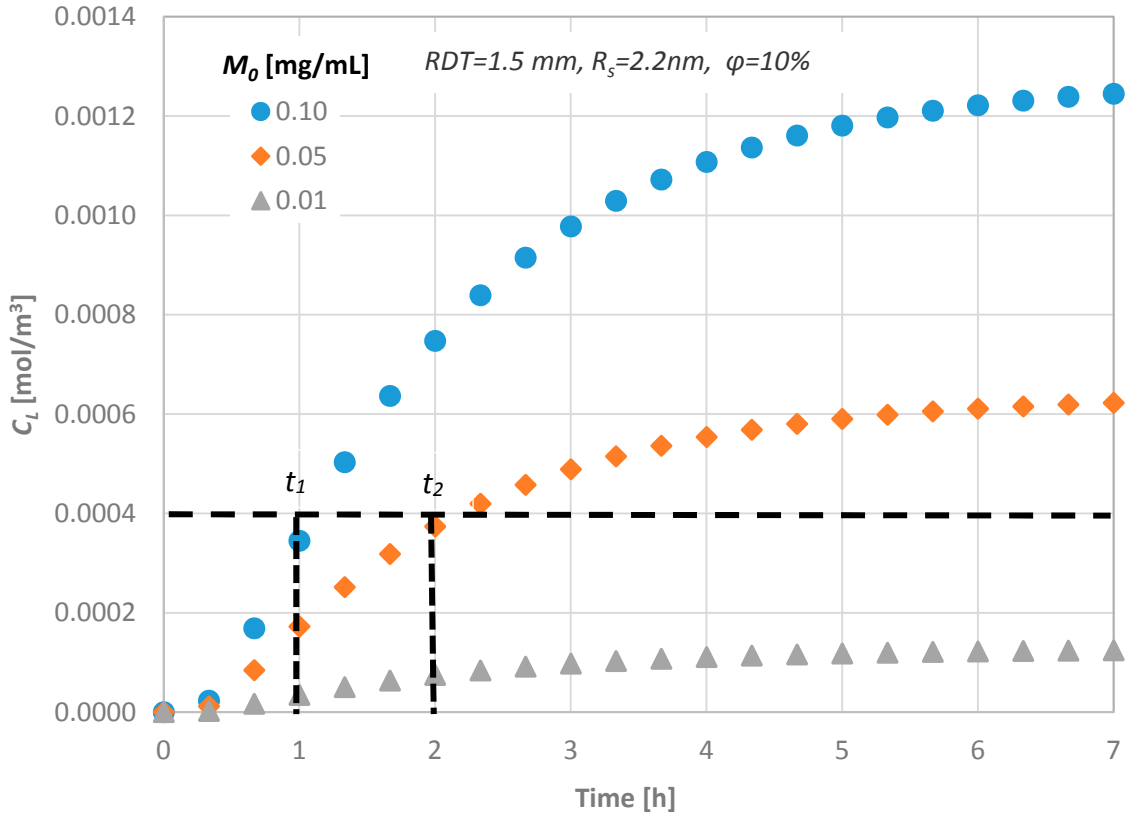

Figure 13: Effect of the initial substance concentration on the diffusion characteristics.

Preprints (www.preprints.org) | NOT PEER-REVIEWED | Posted: 14 November 2017 doi:10.20944/preprints201711.0090.v1

Peer-reviewed version available at Fluids 2018, 3, 4; doi:10.3390/fluids3010004

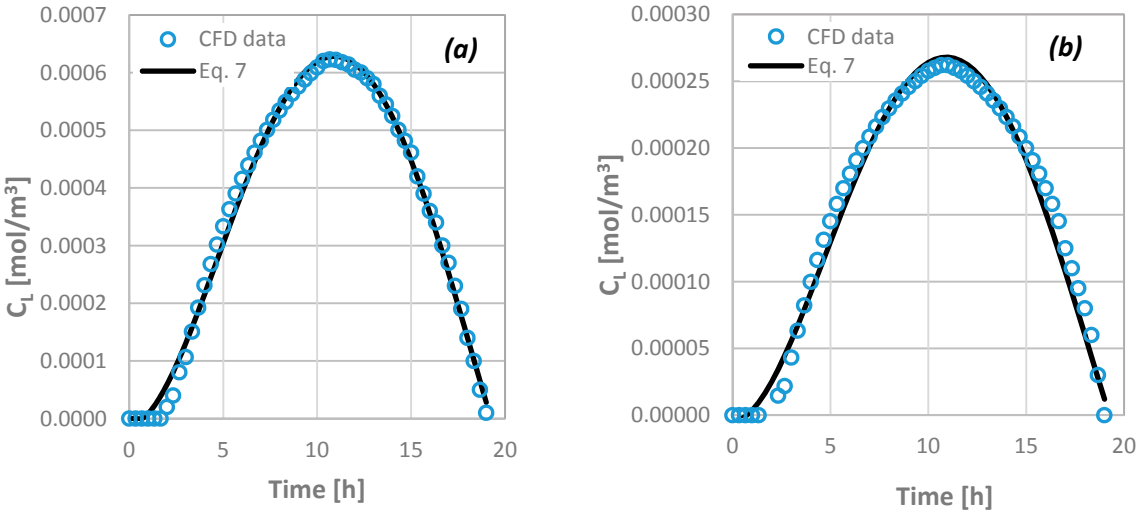

Figure 14: Comparison of CFD data concerning the concentration of agents at the porous disc bottom as a function of time with the outcome of Eq. 7 for: RDT=2.5 mm, ϕ=10%, R_s=2.2 nm; (a) M_0=0.10 and (b) M_0=0.05 mg/mL.

5 Conclusions

This study aims to investigate the key features that affect transdentinal drug delivery and consequently to determine the necessary quantitative and qualitative issues to be addressed before the application of effective treatment modalities in dental clinical practice. These issues are also related to the diffusion of potentially irritating molecules released from restorative materials. The study has been conducted using CFD simulations validated with relevant experimental data acquired by employing the novel, non-intrusive μ-LIF technique. More specifically, the effect of the molecular size and the initial concentration of various compounds on the transdentinal diffusion characteristics were investigated. The geometrical characteristics (i.e. the porosity of the tissue and its thickness) as well as the consumption rate of these agents at the pulpal side were also included in a parametric study based on the Design of Experiments (DOE) methodology.

The computational results reveal that:

- the transdentinal diffusion of drugs is mainly affected by the molecular size and the *RDT*, as it was expected,
- a porosity change of 5% to 20% results to less than ±15% C_L difference,
- a variation of the agent consumption rate at the pulpal side between 0-10^{-10} kg/(m²·s), leads to a 100% C_L decrease, while the consumption time is 18-25 h.

Finally, in the framework of thorough investigation of the physico-chemical and clinical parameters that influence the transdentinal delivery of potential irritating substances or therapeutic biomolecules in non-exposed dentinal cavities, we propose a new model. Given the geometrical characteristics of a dentinal cavity (i.e. porosity & *RDT*) in addition to the type of applied molecules, their critical pulpal concentration and the rate of their consumption at the pulp, the proposed model is able to estimate the initial concentration to be imposed if the desirable critical time of application is known and vice versa.

Acknowledgements: The authors would like to thank the Lab technician Mr. A. Lekkas and Asst. Prof. C. Gogos for the construction and installation of the experimental setup. This research has been co-financed by the EU (ESF) and Hellenic National Funds Program "Education and Lifelong Learning" (NSRF)-Research Funding Program: "ARISTEIA"/"EXCELLENCE" (grand no 1904).

Author Contributions: S.V. Paras and D. Tziafas had the initial conception of this work; S.V. Paras and A.D. Passos designed the experiments; A.D. Passos performed the experiments acquired and analyzed the data and drafted the work; S.V. Paras and A.A. Mouza interpreted the results and revised the manuscript.

Peer-reviewed version available at Fluids 2018, 3, 4; doi:10.3390/fluids3010004

Conflicts of Interest: All authors state that there is **no conflict** of interest.

Nomenclature

C	Molar concentration, mol/m^3
C_L	Molar concentration at the bottom end, mol/m^3
C_o	Initial molar concentration, mol/m^3
C_∞	Final molar concentration (for t=L^2/D), mol/m^3
D	Coefficient of diffusion, m^2/s
j	Concentration flux, mol/m^2·s
L	Length, m
M_0	Mass concentration, g/m^3
M_w	Molecular weight, g/mol
R	Agent consumption rate, kg/(m^2·s)
RDT	Remaining Dentinal Thickness, m
R_s	Stokes radius, m
r	Radius of conduit, m
T	Temperature, C
t^*	Dt/L^2, dimensionless
t	Time, s
U	Velocity, m/s
x	Distance, m
μ	Viscosity, g/cm·s
ϕ	Porosity, %

References

1. De Peralta, T.L.,Nör, J.E. *Regeneration of the living pulp*, in *The Dental Pulp: Biology, Pathology, and Regenerative Therapies*, 2014. p. 237-250.
2. Tziafas, D., Smith, A.J.,Lesot, H. *Designing new treatment strategies in vital pulp therapy.* J Dent 2000, 28, 77-92
3. Rutherford, B., Spangberg, L. *Transdentinal stimulation of reparative dentine formation by osteogenic protein-1 in monkeys.* Arch Oral Biol 1995, 40, 681-3.
4. Kalyva, M., Papadimitriou, S.,Tziafas, D. *Transdentinal stimulation of tertiary dentine formation and intratubular mineralization by growth factors.* Int Endod J 2010, 43, 382-92, 10.1111/j.1365-2591.2010.01690.x.
5. Smith, A.J., Tobias, R.S.,Murray, P.E. *Transdentinal stimulation of reactionary dentinogenesis in ferrets by dentine matrix components.* Journal of Dentistry 2001, 29, 341-346, https://doi.org/10.1016/S0300-5712(01)00020-3.
6. Pashley, D.H. *Dentin permeability: Theory and practice*, CRC Press Inc.:Boca Raton, Florida, 1990.
7. Pashley, D.H. *Dentin permeability and dentin sensitivity.* Proc Finn Dent Soc 1992, 88 Suppl 1, 31-7.
8. Murray, P.E., Smith, A.J. *Remaining dentine thickness and human pulp responses.* International Endodontic Journal 2003, 36, 33-43, 10.1046/j.0143-2885.2003.00609.x.
9. Smith, A.J. *Vitality of the dentin-pulp complex in health and disease: growth factors as key mediators.* Journal of dental education 2003, 67, 678-689.
10. Pashley, D.H.,Matthews, W.G. *The effects of outward forced convective flow on inward diffusion in human dentine in vitro.* Arch Oral Biol 1993, 38, 577-82.
11. Hanks, C.T., Wataha, J.C.,. *Permeability of biological and synthetic molecules through dentine.* J Oral Rehabil 1994, 21, 475-87.
12. Boutsioukis, C., Lambrianidis, T.,Kastrinakis, E. *Irrigant flow within a prepared root canal using various flow rates: a Computational Fluid Dynamics study.* International Endodontic Journal 2009, 42, 144-155, DOI 10.1111/j.1365-2591.2008.01503.x.

13. Gao, Y., Haapasalo, M.,. *Development and Validation of a Three-dimensional Computational Fluid Dynamics Model of Root Canal Irrigation.* Journal of Endodontics 2009, 35, 1282-1287, 10.1016/j.joen.2009.06.018.
14. Su, K.C., Chuang, S.F. *An investigation of dentinal fluid flow in dental pulp during food mastication: Simulation of fluid-structure interaction.* Biomechanics and Modeling in Mechanobiology 2014, 13, 527-535, 10.1007/s10237-013-0514-z.
15. Passos, A.D., Tziafas, D, Mouza, A.A., Paras, S.V. *Study of the transdentinal diffusion of bioactive molecules.* Medical Engineering and Physics 2016, 10.1016/j.medengphy.2016.09.005.
16. Ingle, J.I., Bakland, L.K.,Baumgartner, J.C. *Ingle's Endodontics 6*, BC Decker:Hamilton, Ontario, 2008.
17. Garberoglio, R.,Brannstrom, M. *Scanning electron microscopic investigation of human dentinal tubules.* Arch Oral Biol 1976, 21, 355-62.
18. Andrew, D.,Matthews, B. *Displacement of the contents of dentinal tubules and sensory transduction in intradental nerves of the cat.* J Physiol 2000, 529 Pt 3, 791-802.
19. Fearnhead, R.W. *Histological evidence for the innervation of human dentine.* J Anat 1957, 91, 267-77
20. Hildebrand, C., Fried, K.,. *Teeth and tooth nerves.* Prog Neurobiol 1995, 45, 165-222.
21. Yang, X.L., Liu, Y.,Luo, H.Y. *Respiratory flow in obstructed airways.* Journal of Biomechanics 2006, 39, 2743-2751, DOI 10.1016/j.jbiomech.2005.10.009.
22. Gendron, P.O., Avaltroni, F.,Wilkinson, K.J. *Diffusion coefficients of several rhodamine derivatives as determined by pulsed field gradient-nuclear magnetic resonance and fluorescence correlation spectroscopy.* J Fluoresc 2008, 18, 1093-101, 10.1007/s10895-008-0357-7.
23. Bindhu, C.V.,Harilal, S.S. *Effect of the excitation source on the quantum-yield measurements of rhodamine B laser dye studied using thermal-lens technique.* Analytical Sciences 2001, 17, 141-144, DOI 10.2116/analsci.17.141.
24. Sakakibara, J.,Adrian, R.J. *Whole field measurement of temperature in water using two-color laser induced fluorescence.* Experiments in Fluids 1999, 26, 7-15, 10.1007/s003480050260.
25. Murphy, D.B. *Fundamentals of Light Microscopy and Electronic Imaging*, Wiley, 2002.
26. Mortensen, N.A., Okkels, F.,Bruus, H. *Reexamination of Hagen-Poiseuille flow: Shape dependence of the hydraulic resistance in microchannels.* Physical Review E 2005, 71, 057301.
27. Paterson, M.S. *The equivalent channel model for permeability and resistivity in fluid-saturated rock—A re-appraisal.* Mechanics of Materials 1983, 2, 345-352, https://doi.org/10.1016/0167-6636(83)90025-X.
28. Panda, M.N.,Lake, L.W. *Estimation of Single-Phase Permeability from Parameters of Particle-Size Distribution.* Aapg Bulletin-American Association of Petroleum Geologists 1994, 78, 1028-1039
29. Erickson, H.P. *Size and Shape of Protein Molecules at the Nanometer Level Determined by Sedimentation, Gel Filtration, and Electron Microscopy.* Biological Procedures Online 2009, 11, 32-51, 10.1007/s12575-009-9008-x.
30. Kishen, A.,Vedantam, S. *Hydromechanics in dentine: role of dentinal tubules and hydrostatic pressure on mechanical stress-strain distribution.* Dent Mater 2007, 23, 1296-306, 10.1016/j.dental.2006.11.018.
31. Stogiannis, I.A., Mouza, A.A., Paras, S.V. *Study of a micro-structured PHE for the thermal management of a fuel cell.* Applied Thermal Engineering 2013, 59, 717-724, https://doi.org/10.1016/j.applthermaleng.2012.08.024.
32. Outhwaite, W.C., Livingston, M.J., Pashley, D.H. *Effects of changes in surface area, thickness, temperature and post-extraction time on human dentine permeability.* Arch Oral Biol 1976, 21, 599-603.